

MUON SHIELD  
for the  
TEVATRON at FERMILAB

S.Mori

May 17, 1978

I. Introduction

The present muon shield arrangement for the neutrino beams at Fermilab was designed for 500 GeV and consists mainly of soil. It requires a substantial modification for the Tevatron operation at 1000 GeV.<sup>1</sup> A Monte Carlo program was used to calculate muon backgrounds at the 15-Foot Bubble Chamber for various shield configurations. The present layout of the target tube, decay pipe and the 15-Foot Bubble Chamber are kept unchanged. Only passive shielding by iron and soil combination was considered in the present study.

Energy loss processes used are mainly atomic collisions and pair productions. Although energy losses due to bremsstrahlungs and nuclear interactions become significant in the Tevatron energy region, these processes may cause large fluctuations. Effects from bremsstrahlungs will be discussed.

Three shield arrangements which provide roughly ten background muons per square meter for  $10^{13}$  incident protons at the 15-Ft. Bubble Chamber will be discussed: (1) iron shield after the decay pipe, (2) iron shield around and after the decay pipe, and (3) iron shield inside and after the decay pipe.

II. Input Parameters

A. Energy Loss,  $dE/dx$

The most important parameters in designing a muon shield are the energy loss rate,  $dE/dx$ , of high energy muons and multiple Coulomb scattering. G.Koizumi<sup>2</sup> calculated energy

losses for muons produced in the Tevatron energy region. The  $dE/dx$  results for iron and soil are reproduced in Figure 1. We consider two cases: (1) energy losses due to atomic collisions and pair productions, and (2) energy losses due to atomic collisions, pair productions, and bremsstrahlungs. The energy loss which includes nuclear interactions will not be considered.

B. Multiple Coulomb Scattering<sup>3</sup>

We consider only multiple Coulomb scattering for angular scattering of muons and assume a Gaussian distribution. The average scattering angle is given by

$$\langle \theta^2 \rangle_{\text{ave}}^{1/2} = \frac{0.021}{P} \times X^{1/2}$$

where  $X$  is measured in radiation lengths and  $P$  is the muon momentum in GeV/c. In order to estimate the effect due to large angle scattering, muon backgrounds were also calculated for large average scattering angles.

C. Production of Parent Particles of Muons

The primary source of high energy muons is the decay of positive pions. Muons from kaon decays have energies less than 450 GeV and are totally ranged out for any shield configurations considered in the present study. Any other processes have been neglected. R.Stefanski/H.White's parametrization<sup>4</sup> was used for pion production. Figure 2 shows the integrated positive pion yield as a function of the pion energy. The incident proton energy is 1000 GeV. As will be seen later, pions produced with production angles greater than 5 mrad are very unlikely to contribute to muon backgrounds for any shield configurations and are not included in the integration.

D. Focussing Properties of Neutrino Beams

When positive pions are focussed parrallel for the neutrino beams, muon backgrounds from the positive pion decays are smaller than from the bare target beam in which pions are not

focussed, as will be seen later. The antineutrino horn beam, in which positive pions are defocussed and appear as if they were produced with larger angles, seem to cause the largest muon background among all the neutrino beams which have been considered so far for the Tevatron. We use primarily the bare target beam for calculations of the muon backgrounds. Effects from the antineutrino horn beam will be discussed separately.

### III. Muon Shields

#### A. Iron Shield After the Decay Pipe

Figure 3 shows the schematic diagram of the simplest shield arrangement which requires installation of a single block of iron shield after the decay pipe. (This iron shield will be called simply the iron shield hereafter.) No modification to the present decay pipe is required. For ease of computation we assume that the decay pipe with the radius of 0.45m starts from the target to the upstream end of the iron shield and that the wall thickness of the decay pipe is negligible. We also assume that the iron and soil shields are cylindrically symmetric. Although the distance between the downstream end of the decay pipe and the 15-Ft. Bubble Chamber is about 1000m, we use the effective total shield length of 800m since some enclosures and the Wonder Building area can not be filled with the shielding material. The radius of soil shield is assumed to be 5m.

Computed numbers of muon backgrounds per square meter for  $10^{13}$  incident protons at the 15-Ft. Bubble Chamber as a function of the iron shield radius are shown in Figure 4. The values were averaged over the radius of 5m at the end of the soil shield. Dotted points correspond to the case in which only atomic collisions and pair productions are considered. An iron shield 250m long is required to stop 1000 GeV muons which go through the whole length of the iron shield. Circle points correspond to the case in which the energy loss due

to the Bremsstrahlung process is added. The latter case requires the iron shield length to be only 150m. The lines are to guide the eye and error bars indicate statistical errors in the Monte Carlo calculations throughout the present study.

Triangle points shown in Figure 4 are muon backgrounds computed for the 1.5 times larger average multiple scattering angle than the normal value. As expected, the backgrounds increase by a factor of about two. Details of this effect will be discussed later.

Radial distributions of muon backgrounds for the iron shield radii of 1.25, 1.50, 1.75, and 2.00m are shown in Figure 5. Only energy losses due to atomic collisions and pair productions are considered. The muon backgrounds have minima at the radius of zero due to the shadowing effect from the iron shield. The backgrounds near the radius of 5m cannot be realistic since muons which reach the shield radius of 5m are assumed to disappear totally in the calculations.

In this arrangement the iron shield radius must be 1.8m or larger in order to reduce muon backgrounds to less than 10 muons per square meter for  $10^{13}$  incident protons. When the energy loss due to the Bremsstrahlung process is included, the muon backgrounds are substantially reduced.

Although the energy losses due to bremsstrahlung and nuclear interaction processes are very important at higher energies, they can cause large fluctuations. Therefore, it seems to be reasonable to use the energy losses due to atomic collisions and pair productions in estimating the radius of the iron shield.

#### B. Iron Shields Around and After the Decay Pipe

In this section we study the shield arrangement in which iron shielding surrounds a part of the decay pipe in addition to the iron shield after the decay pipe. The decay pipe

aperture of 0.45m will not be changed in order to retain the neutrino fluxes which are presently available. This arrangement can allow us to reduce the total amount of iron required for the muon shield described in the previous section. Only energy losses due to atomic collisions and pair productions are used in this section and the following section.

The energy and production angle correlation of positive pions which are produced at the target and yield muon backgrounds at the neutrino detector is shown in Figure 6. The radius of the iron shield is 1.5m, and no decay pipe iron shield is used. It can easily be seen that most of the background muons are caused by pions produced in the angular range between 2 and 5 mrad. Small contribution comes from very high energy pions above 800 GeV with production angles from 1 to 2 mrad. Pions produced with angles larger than 5 mrad do not appreciably contribute to the background. Therefore, iron shielding around the decay pipe and near the target should be very ineffective. The schematic drawing of a desirable shield arrangement is shown in Figure 7. Since the thickness and length of the decay pipe iron shield complement each other, we use a fixed length of 300m and vary the thickness.

Figure 8 shows a plot of the energy and production angle correlation of pions similar to that shown in Figure 6. The outer radius of the decay pipe iron shield of Figure 8 is 0.65m; i.e., the thickness of the decay pipe iron shield is 0.20m. The muon background is suppressed dramatically by the decay pipe iron shield.

Radial distributions of muon backgrounds as a function of the outer radius of the decay pipe iron shield are shown in Figures 9, 10, and 11, for the iron shield radii of 1.5, 1.25, and 1.00m, respectively. When the iron shield radius becomes 1m or less, any additional decay pipe iron shield can not provide sufficient shielding. Scatter plots of energy and production angle correlations of pions which yield muon back-

grounds are shown in Figures 12 and 13 for the iron shield radii of 1.25 and 1.00m. The outer radii of the decay pipe iron shield are 0.75 and 1.00m. For the iron shield radius of 1m a large fraction of the muon backgrounds comes from pions which are produced within 1 mrad and do not intersect the decay pipe.

The smaller the iron shield radius is, the larger the muon background due to large angle scattering. To see this effect a scatter plot of energy and angle correlation of pions is shown in Figure 14 for the iron shield radius of 1.25m and the outer radius of the decay pipe iron shield of 0.75m with a 1.5 times larger average multiple scattering angle (smearing factor = 1.5). Background contribution from pions produced within 1 mrad becomes substantially larger. (See the triangle points shown in Figure 9.)

For the shield arrangement described in this section the iron shield radius of 1.25m and the decay pipe iron shield outer radius of 0.75m seem to be marginally acceptable when we consider the effect due to large angle scattering.

C. Iron Shields Inside and After the Decay Pipe

Figure 15 shows the schematic diagram of the shield arrangement in which an iron shield is added inside the decay pipe. This shield arrangement reduces low energy neutrino fluxes for some of the neutrino beams. To minimize this effect the decay pipe iron shield must be placed at the upstream part of the decay pipe. Computed radial distributions of muon backgrounds are shown in Figure 16 for the iron shield radii of 1.00, 1.25, and 1.50m. The inner radius and length of the decay pipe iron shield are 0.225m and 200m, respectively. The iron shield radius of 1.50m can provide an adequate shield. The total amount of iron is substantially less compared to the shield arrangement shown in Figure 3.

#### IV. Neutrino Beams and Muon Backgrounds

As discussed in the previous chapter, high energy pions ( $>500$  GeV) produced with large angles ( $\gtrsim 1$  mrad) constitute the principal source of muon backgrounds. Therefore, when high energy pions are focussed parallel or absorbed before decaying, they do not yield muon backgrounds provided that the iron shield after the decay pipe is long enough to range out muons which go straight through the iron shield without being scattered out from the side of the iron shield.

The antineutrino horn beam seems to give the most serious muon backgrounds. (See Section II (C).) Computed radial distributions of muon backgrounds for the bare target beam and the antineutrino horn beam are shown in Figure 17 for the two shield arrangements. The antineutrino horn beam is assumed to defocus positive pions by  $0.3$  GeV/c in the transverse direction.<sup>5</sup> The background for the antineutrino beam are worse by a factor of about 3.

Although the decay of negative pions is less serious because of smaller production cross section compared to positive pions, the neutrino horn beam can yield large muon backgrounds from negative pion decay.

We have neglected pions produced with angles greater than 5 mrad. When pions with large production angles are focussed parallel, they can contribute to the background. However, since fewer pions are <sup>produced</sup> with large angles and high energy, their background contribution cannot be serious.

#### V. Conclusions

Table II summarizes radii, lengths, and weights of the iron shields and decay pipe iron shields that can provide muon backgrounds of 10 muons per square meter for  $10^{13}$  incident protons at the 15-Ft. Bubble Chamber. The incident proton energy is 1000 GeV. The length of the iron shield depends strongly upon the  $dE/dx$  used in the calculations. If the energy loss due to the bremsstrahlung or nuclear interaction processes can be

included, the length can be substantially shorter. On the other hand the radius of the iron shield needed is relatively insensitive to the processes considered as seen from Figure 4, in which the bremsstrahlung process is included in the  $dE/dx$ , but not in the angular scattering. Since the bremsstrahlung and nuclear interaction processes are subject to large fluctuations, it seems to be reasonable to use only the losses due to atomic collisions and pair productions in determining the radius of the iron shield. Two sets of values given in Table II for the lengths and weights of the iron shield correspond to the cases without and with the energy loss due to the bremsstrahlung process. The nuclear interaction process has not been considered in the present study.

In designing the muon shield in the new energy region, there always remain several unknown factors which cannot be solved before construction is completed. Focussing by the neutrino beams and large angle scattering can increase muon backgrounds as discussed in the previous sections. Production cross section of pions for the 1000 GeV proton is not well established. How the bremsstrahlung and nuclear interaction processes effect the design parameters is uncertain.

It is certainly easy to make a safer conservative design, but the cost becomes prohibitively expensive for the Tevatron. The arrangement II(A) requires the large amount of iron, but construction is simple. The arrangement II(B) uses the least amount of iron, but modifications of the decay pipe will be expensive.

Valuable discussions with G.Koizumi, W.Nestander, and D.Theriot are greatly acknowledged.



References

1. Some studies about the Tevatron Muon shielding were discussed in the 1976 Summer Study Report, 1976 (Fermilab Report).
2. G.Koizumi, Muon  $dE/dx$  and Range Tables for Tevatron Energies, Fermilab Internal Report, TM-786, May, 1978.
3. D.M. Ritson, Technology of High Energy Physics, Interscience Publishers, Inc., New York, 1961.
4. R.Stefanski and H.White, Jr., Neutrino Flux Distributions, Fermilab Internal Report, FN-292, 1976.
5. S.Mori, Wide-Band Single Horn System(II), Fermilab Internal Report, TM-720, 1977.

FIGURE CAPTIONS

1.  $dE/dx$  For Iron and Soil. Two cases are shown in which the energy losses are due to (1) atomic collisions and pair productions and due to (2) atomic collisions, pair productions, and bremsstrahlungs.
2. Integrated positive pion yield for  $\theta_{\text{prod}} < 5$  mrad. The incident proton energy is 1000 GeV and Stefanski-White's parametrization is used for pion production.
3. Schematic drawing for the muon shield arrangement in which iron shielding is used only after the decay pipe and in which no modification to the decay pipe is required.
4. Computed muon backgrounds per square meter for  $10^{13}$  1000 GeV incident protons as a function of the iron shield radius. The values are averaged over the radius of 5m at the end of soil shield. Dotted points correspond to the case in which only atomic collisions and pair productions are considered and circle points to the case in which the energy loss due to bremsstrahlungs is added. Triangle points are muon backgrounds for the 1.5 times larger average multiple scattering angle than the normal value. The lines are to guide the eye and the error bars indicate statistical errors in the Monte Carlo calculations.
5. Radial distributions of muon backgrounds for the iron shield radii of 1.25, 1.50, 1.75, and 2.00m. No decay pipe iron shield is used.
6. Energy and production angle correlation of positive pions which yield muon backgrounds. The iron shield radius is 1.50m and no decay pipe iron shield is used.
7. Schematic drawing for the muon shield arrangement in which iron shielding is used around and after the decay pipe.
8. Energy and production angle correlation of positive pions

which yield muon backgrounds. The iron shield radius is 1.50m and the decay pipe iron shield outer radius is 0.65m.

9. Radial distributions of muon backgrounds for the iron shield radius of 1.5m and the decay pipe iron shield outer radii of 0.45, 0.55, 0.65, and 0.75m.
10. Radial distributions of muon backgrounds for the iron shield radius of 1.25m and the decay pipe iron shield outer radii of 0.45, 0.55, 0.65, and 0.75m
11. Radial distributions of muon backgrounds for the iron shield radius of 1.0m and the decay pipe iron shield outer radii of 0.75m and 1.0m.
12. Energy and production angle correlation of positive pions which yield muon backgrounds. The iron shield radius is 1.25m and the decay pipe iron shield outer radius is 0.75m.
13. Energy and production angle correlation of positive pions which yield muon backgrounds. The iron shield radius is 1.0m and the decay pipe iron shield outer radius is 1.0m.
14. Energy and production angle correlation of positive pions which yield muon backgrounds. The iron shield radius is 1.25m and the decay pipe iron shield outer radius is 0.75m. The 1.5 times larger average scattering angle than the normal value is used (smearing factor = 1.5).
15. Schematic drawing for the muon shield arrangement in which iron shielding is used inside and outside the decay pipe.
16. Radial distributions of muon backgrounds for the iron shield radii of 1.00, 1.25, and 1.50m. The inner radius and length of the decay pipe iron shield is 0.225m and 200m, respectively.
17. Radial distributions of muon backgrounds for the bare target beam and the antineutrino horn beam. The iron shield radius is 1.5m and 1.25m.

Table I. Radiation Lengths And Densities Of Iron And Soil.

Substance	Radiation Length ( cm )	Density ( g/cm <sup>3</sup> )
Iron	1.77	7.87
Soil	16.5	1.7

Table II. Radii, Lengths, And Weights Of The Iron Shields And  
 Decay Pipe Iron Shields.

Configu- ration	Iron Shield			Decay Pipe Iron Shield			Total Weight (10 <sup>3</sup> Tons)
	Radius (m)	Length (m)	Weight (10 <sup>3</sup> Tons)	Outer Or Inner Radius (m)	Length (m)	Weight (10 <sup>3</sup> Tons)	
II(A)	1.80	250/150	20.0/12.0	-	-	-	20.0/12.0
II(B)	1.25	250/150	9.7/ 5.8	0.75	300	2.7	12.3/ 8.5
II(C)	1.50	250/150	13.9/ 8.3	0.225	200	0.9	14.8/ 9.3

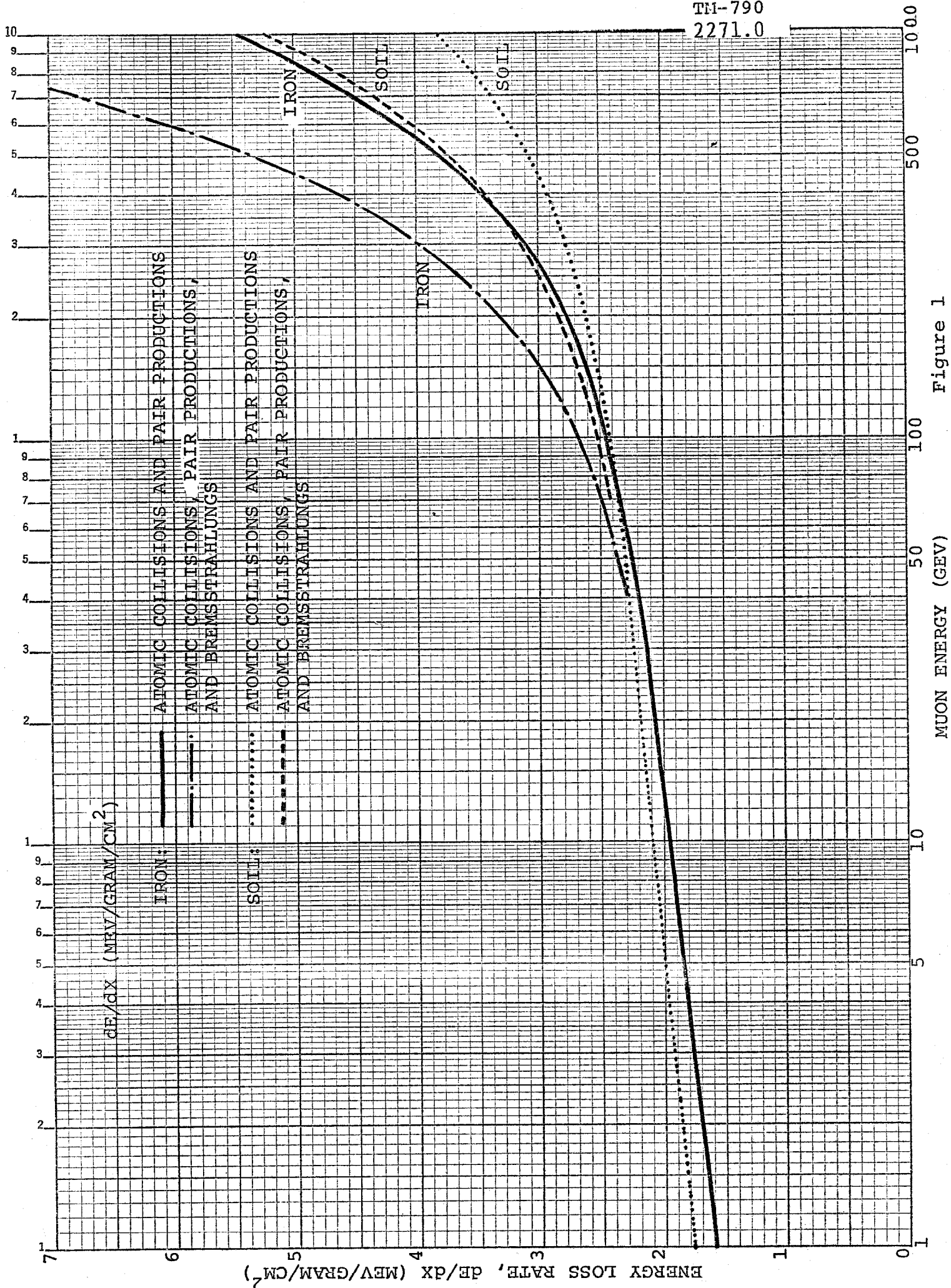


Figure 1

MUON ENERGY (GEV)

## PRODUCTION OF POSITIVE PIONS

INCIDENT PROTON ENERGY = 1000 GEV

STEFANSKI-WHITE'S PARAMETRIZATION USED

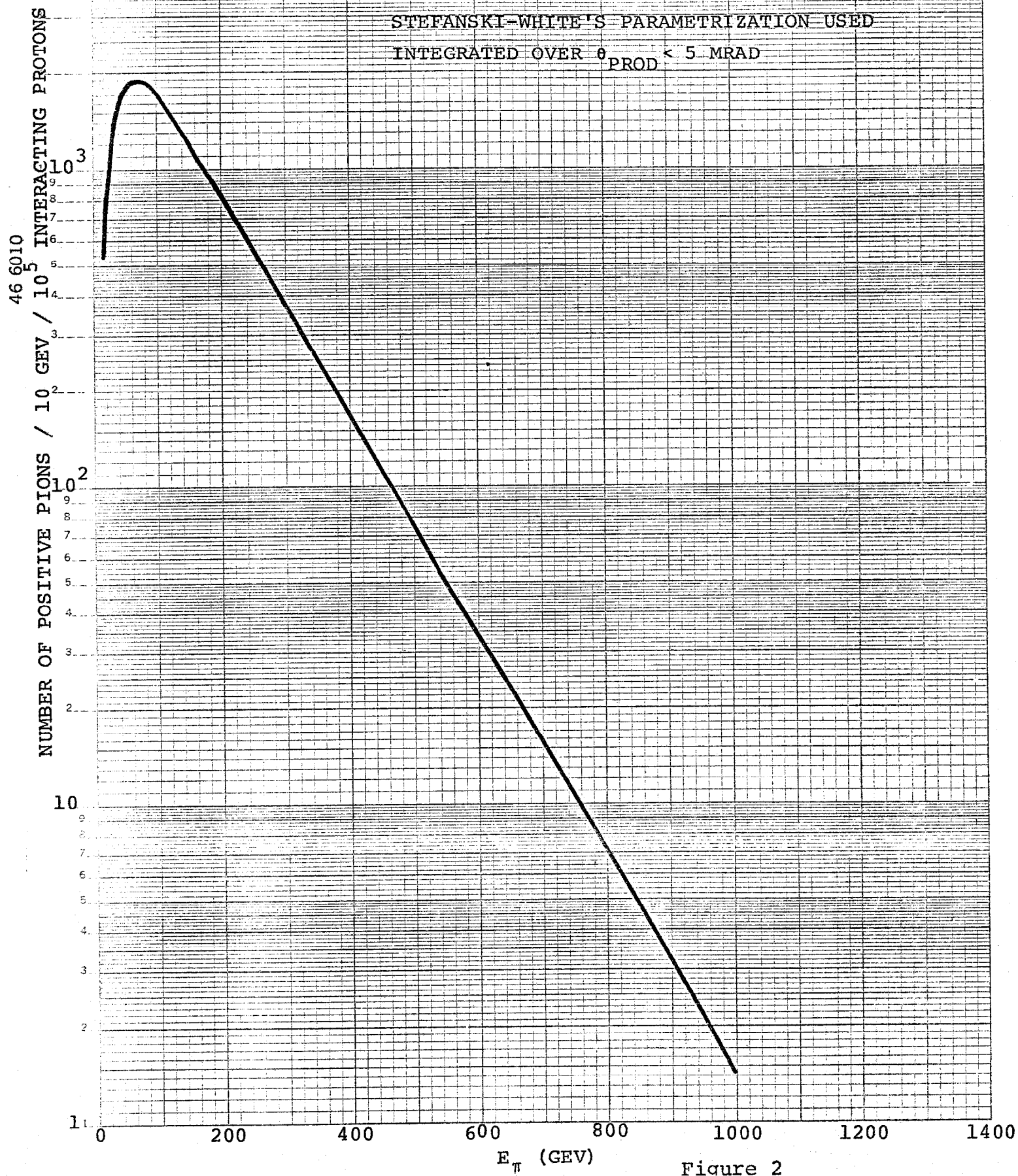
INTEGRATED OVER  $\theta_{\text{PROD}} < 5 \text{ MRAD}$ 

Figure 2

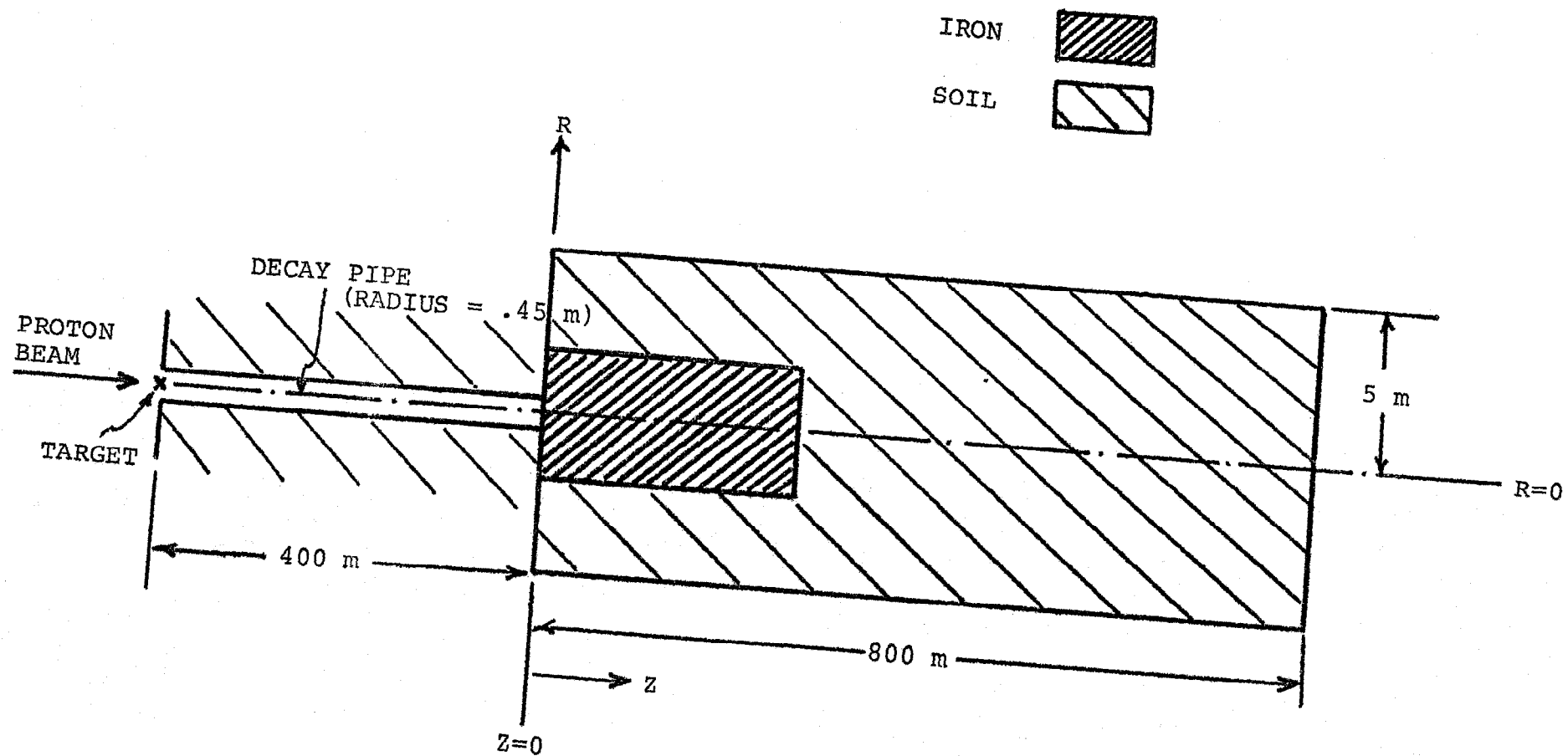


Figure 3

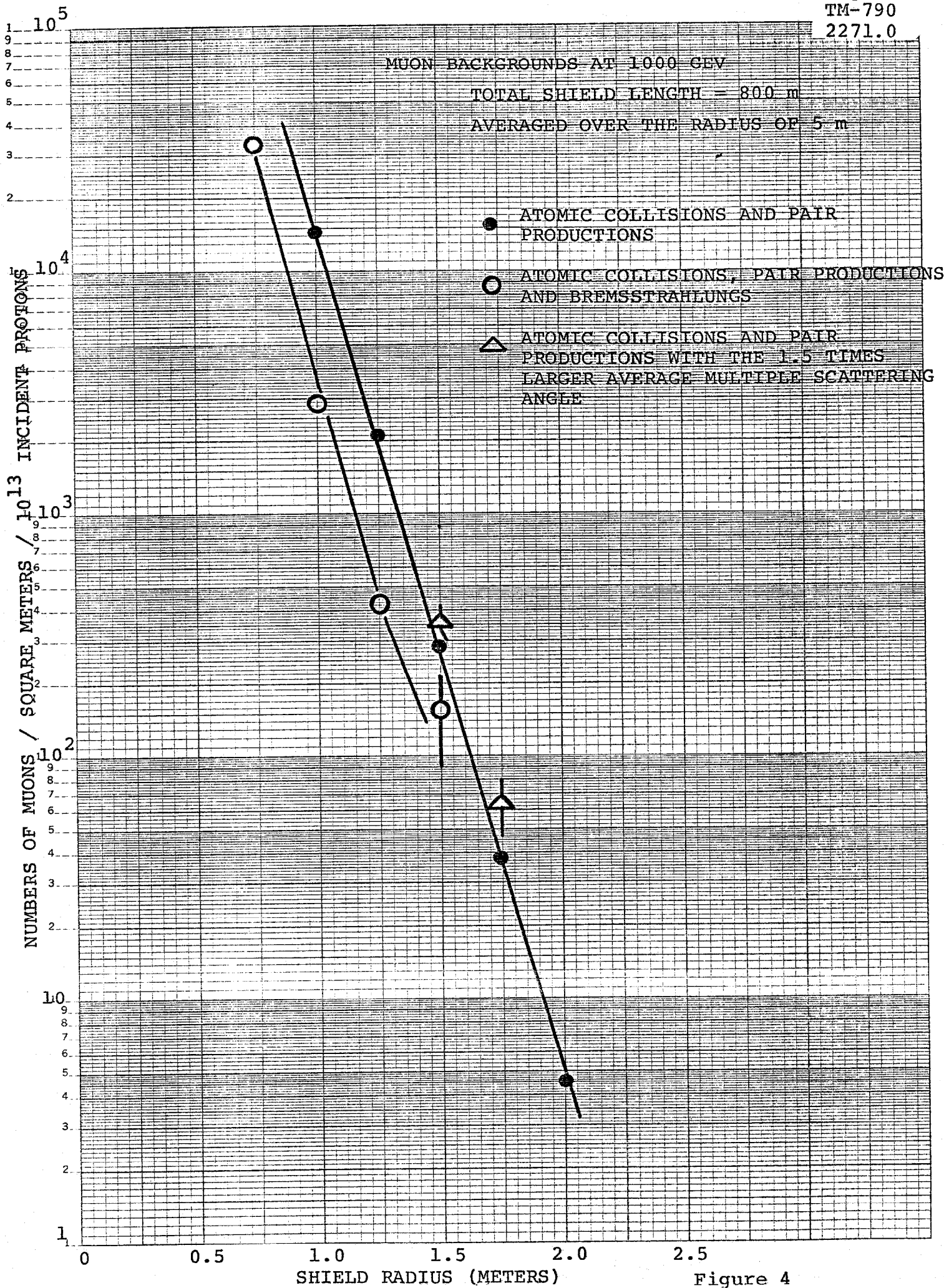


Figure 4



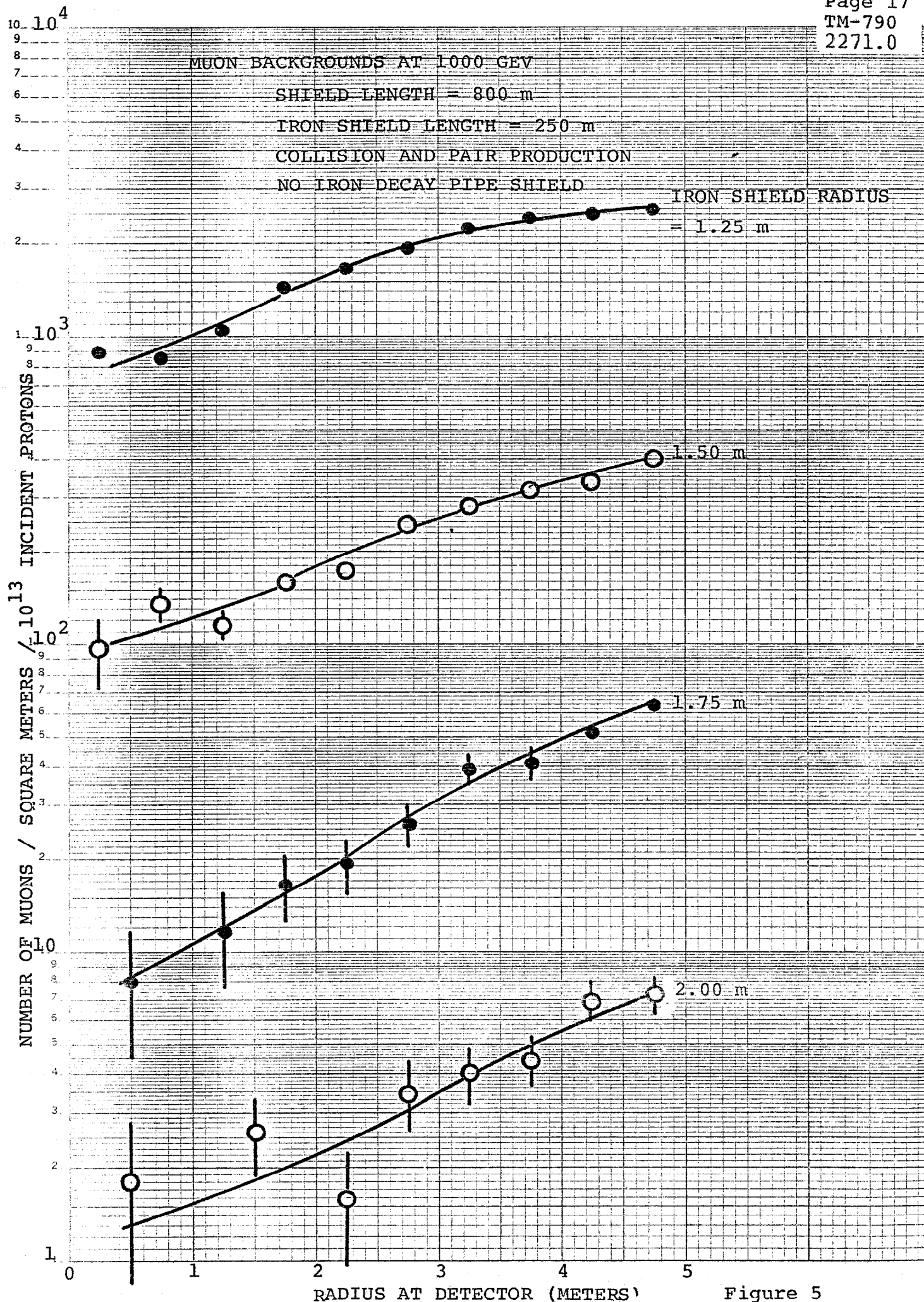


Figure 5

ENERGY AND PRODUCTION ANGLE CORRELATION OF PIONS  
WHICH YIELD MUON BACKGROUNDS AT THE DETECTOR

Page 18  
TM-790  
2271.0

RADIUS OF IRON SHIELD = 1.50 m  
NO DECAY PIPE IRON SHIELD

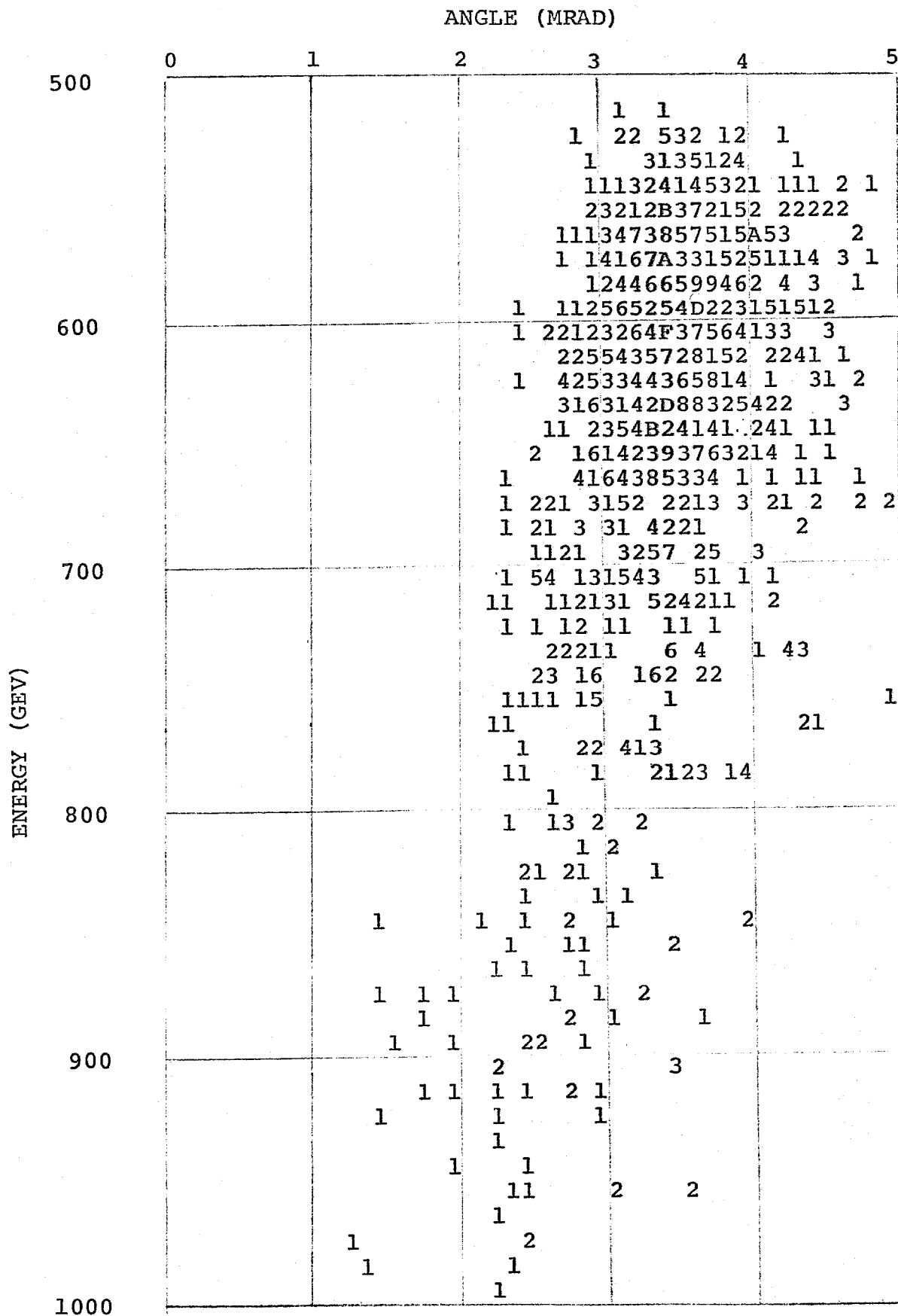


Figure 6

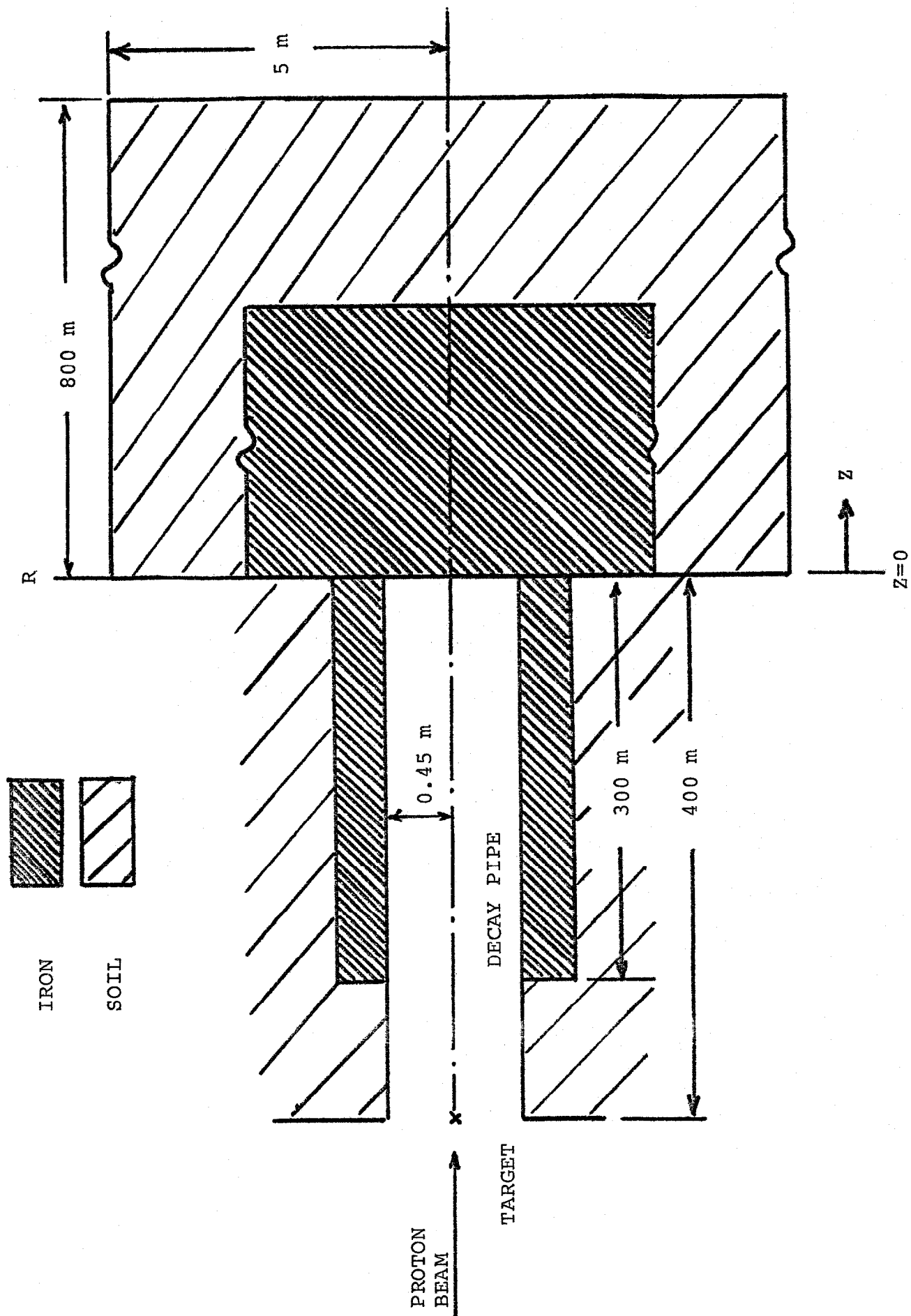


Figure 7

# ENERGY AND PRODUCTION ANGLE CORRELATION OF PIONS WHICH YIELD MUON BACKGROUNDS AT THE DETECTOR

RADIUS OF IRON SHIELD = 1.50 m  
 OUTER RADIUS OF DECAY PIPE IRON SHIELD = 0.65 m

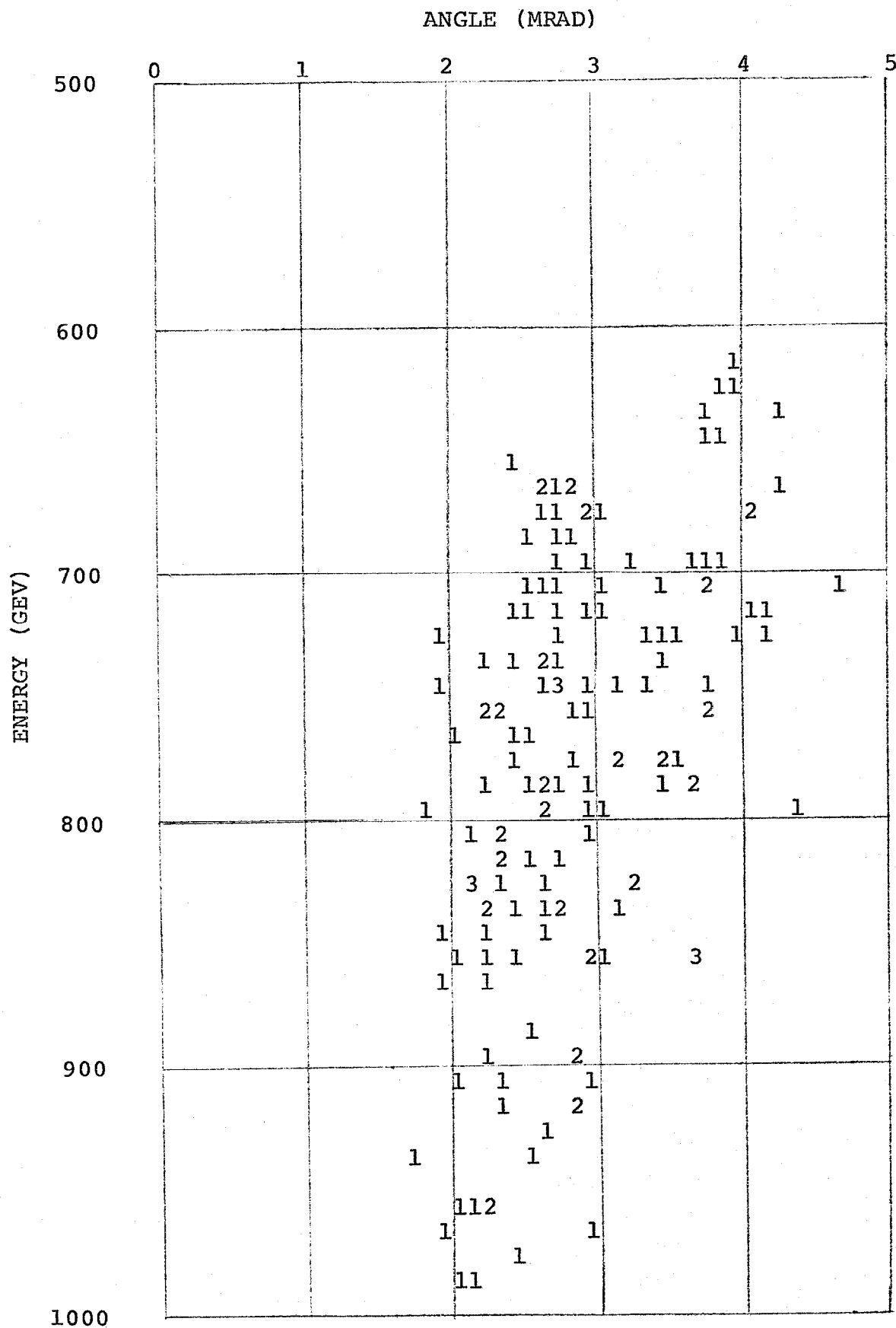


Figure 8

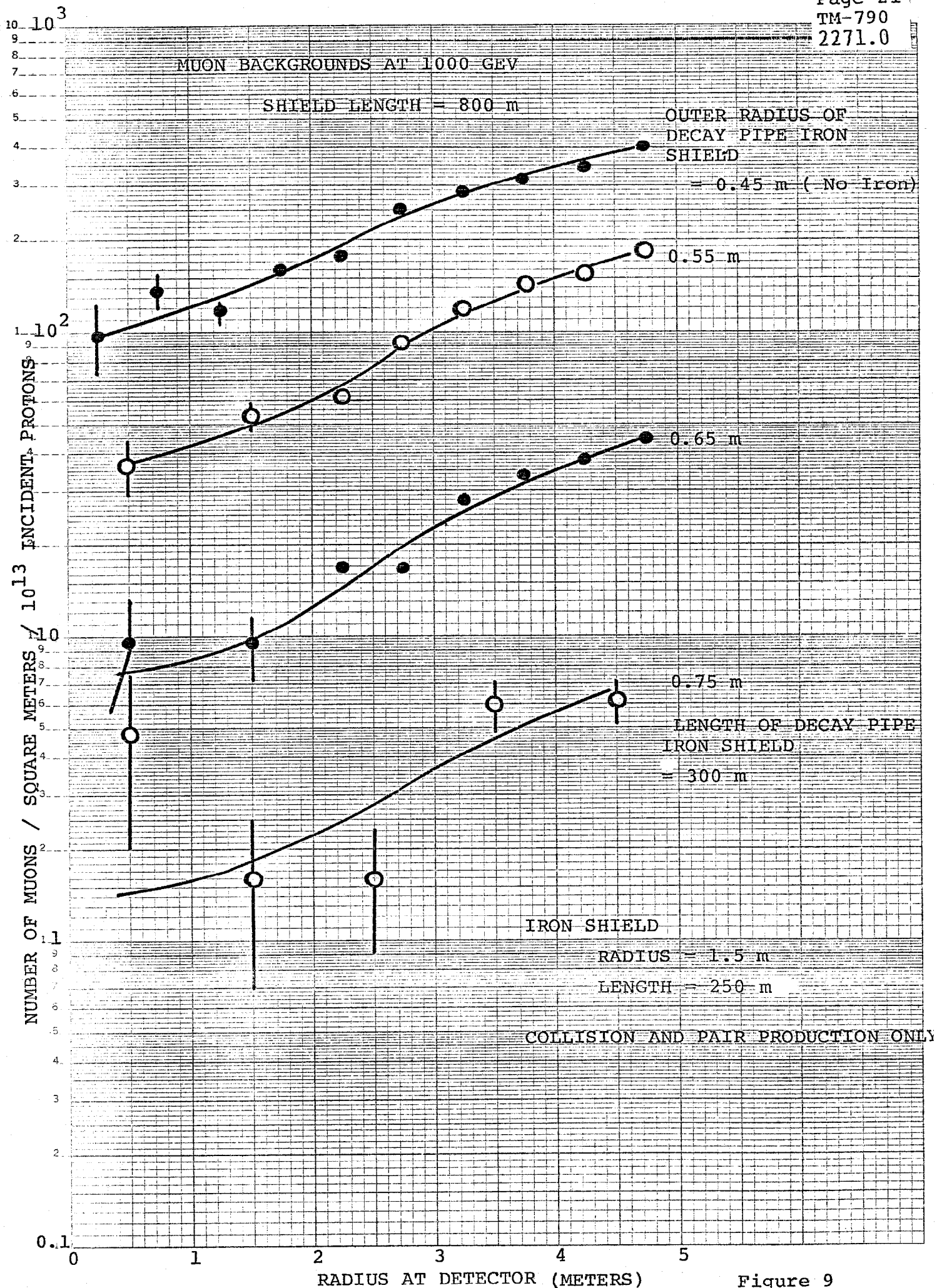


Figure 9

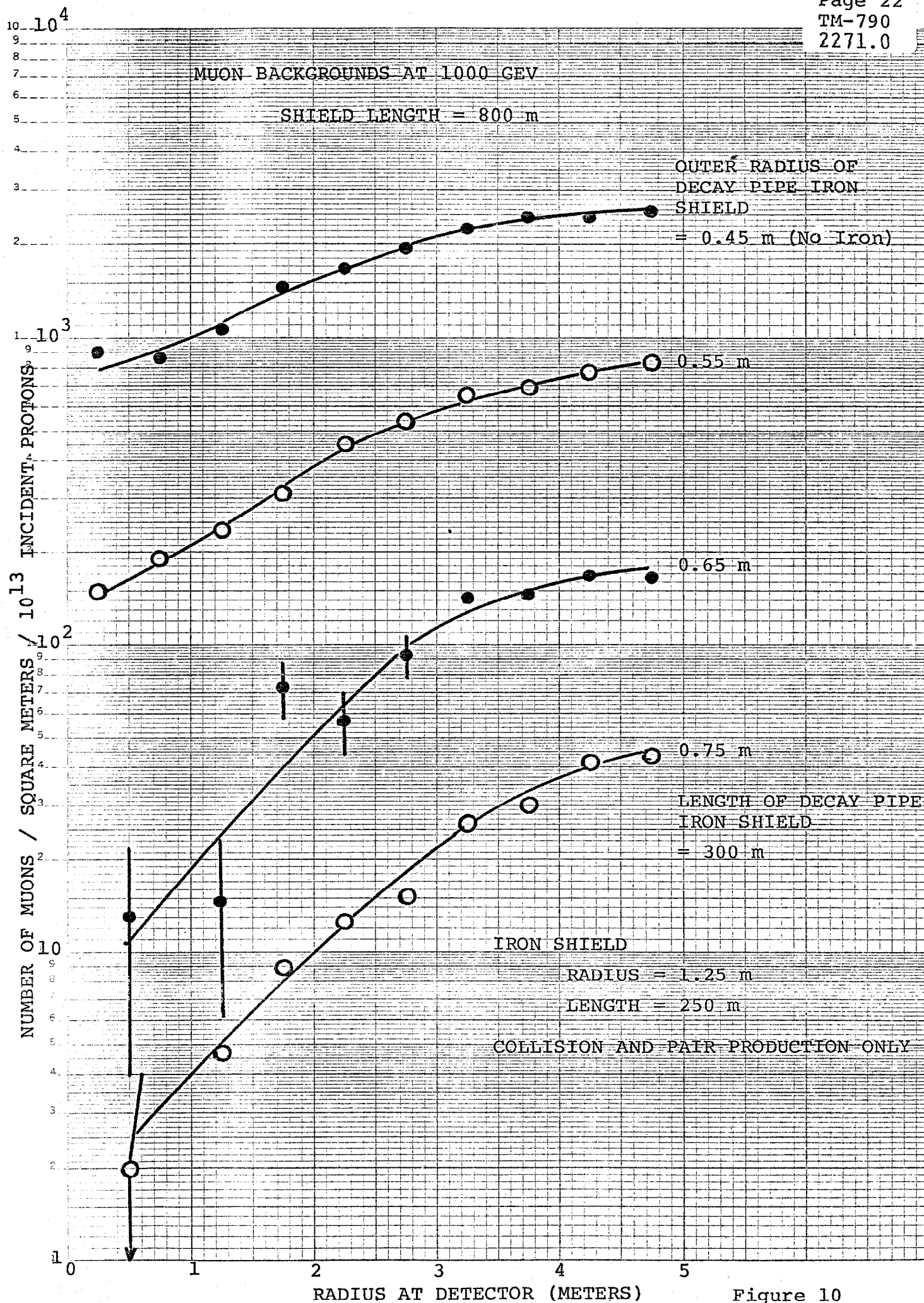


Figure 10



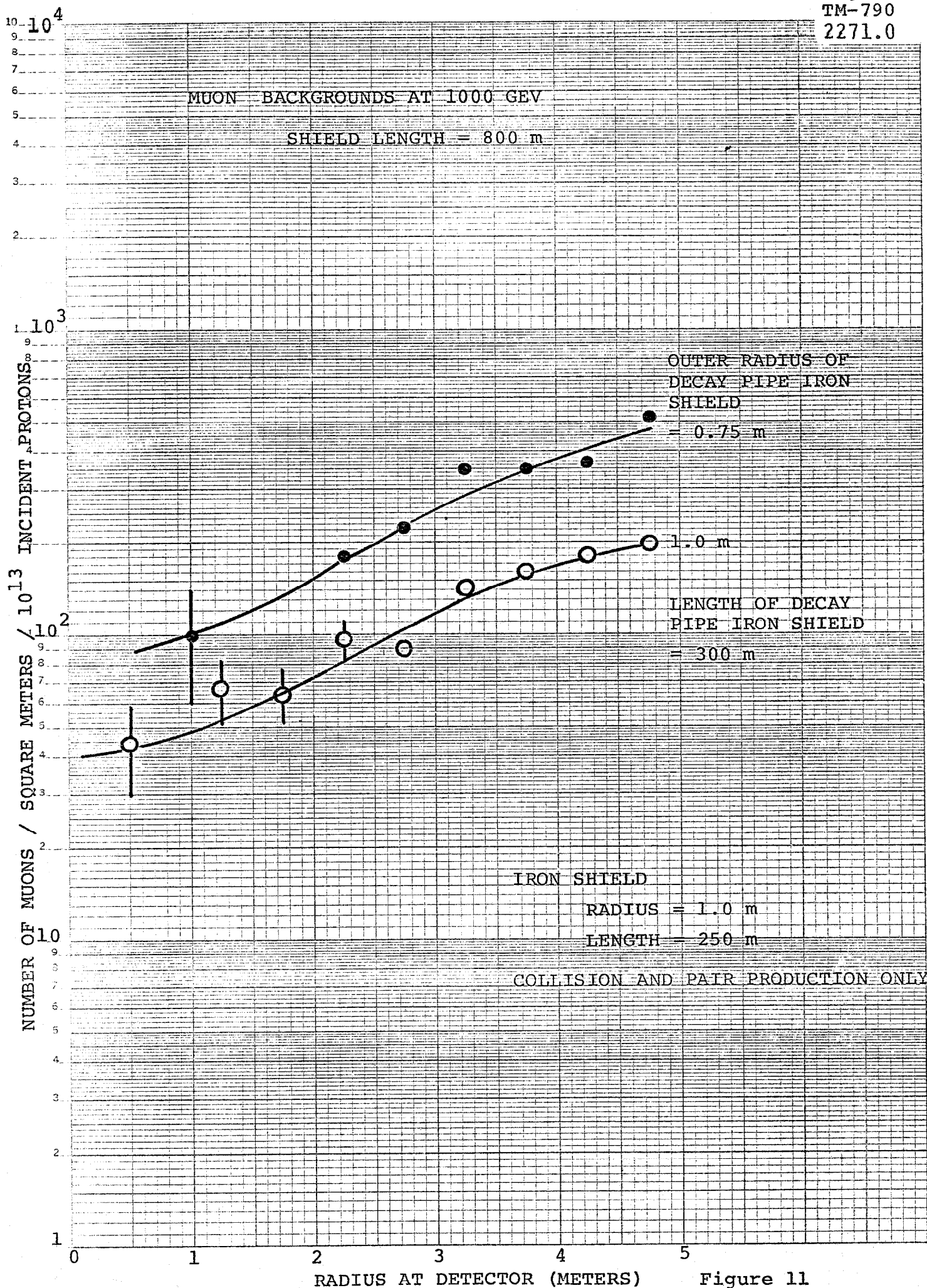
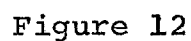


Figure 11

RADIUS OF IRON SHIELD = 1.25 m  
OUTER RADIUS OF DECAY PIPE IRON SHIELD = 0.75 m  
ANGLE (MRAD)





ENERGY AND PRODUCTION ANGLE CORRELATION OF PIONS  
 WHICH YIELD MUON BACKGROUNDS AT THE DETECTOR

RADIUS OF IRON SHIELD = 1.00 m  
 OUTER RADIUS OF DECAY PIPE IRON SHIELD = 1.00 m

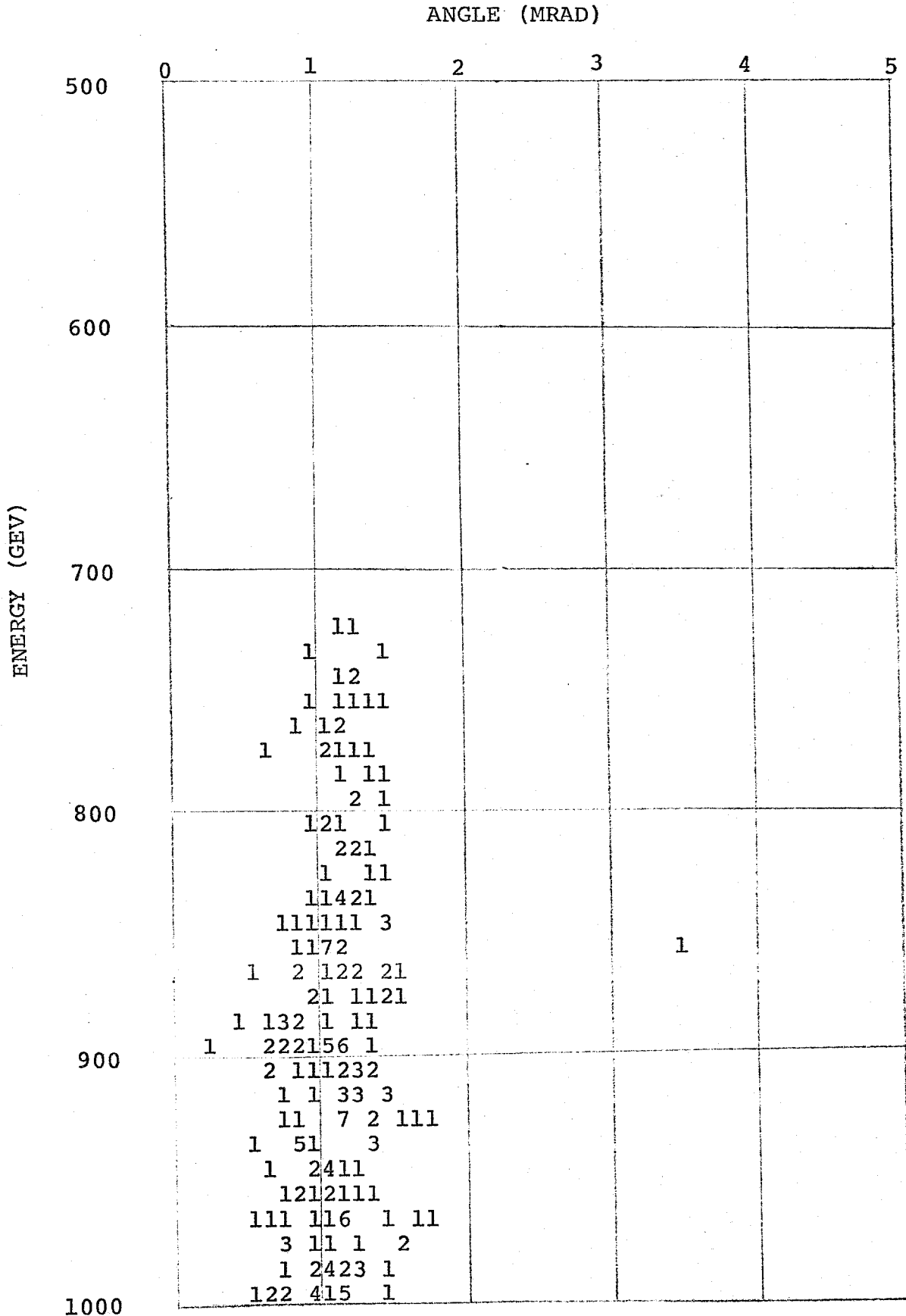


Figure 13

ENERGY AND PRODUCTION ANGLE CORRELATION OF PIONS  
WHICH YIELD MUON BACKGROUNDS AT THE DETECTOR.

Page 26  
TM-790  
2271.0

RADIUS OF IRON SHIELD = 1.25 m  
OUTER RADIUS OF DECAY PIPE IRON SHIELD = 0.75 m

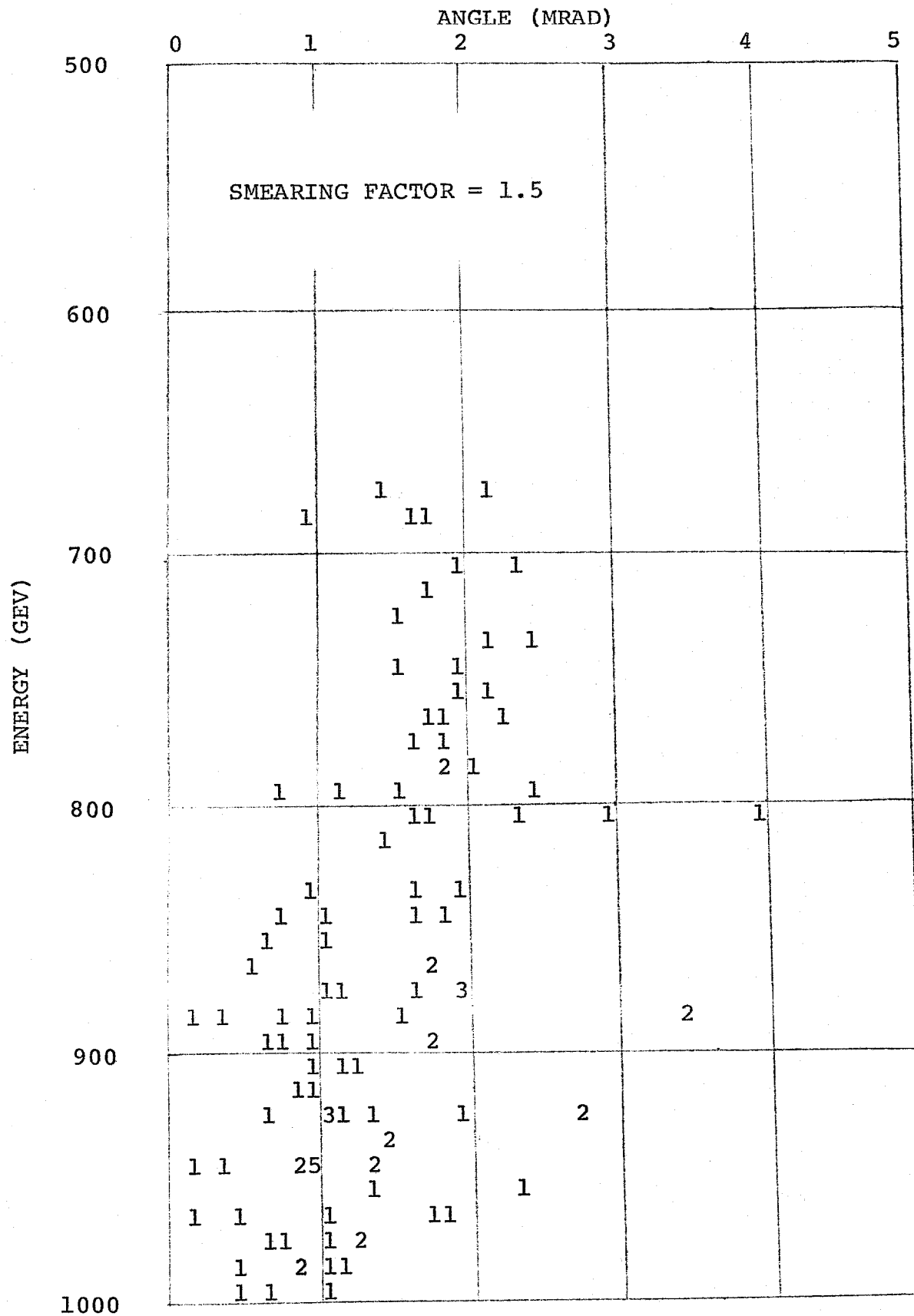


Figure 14

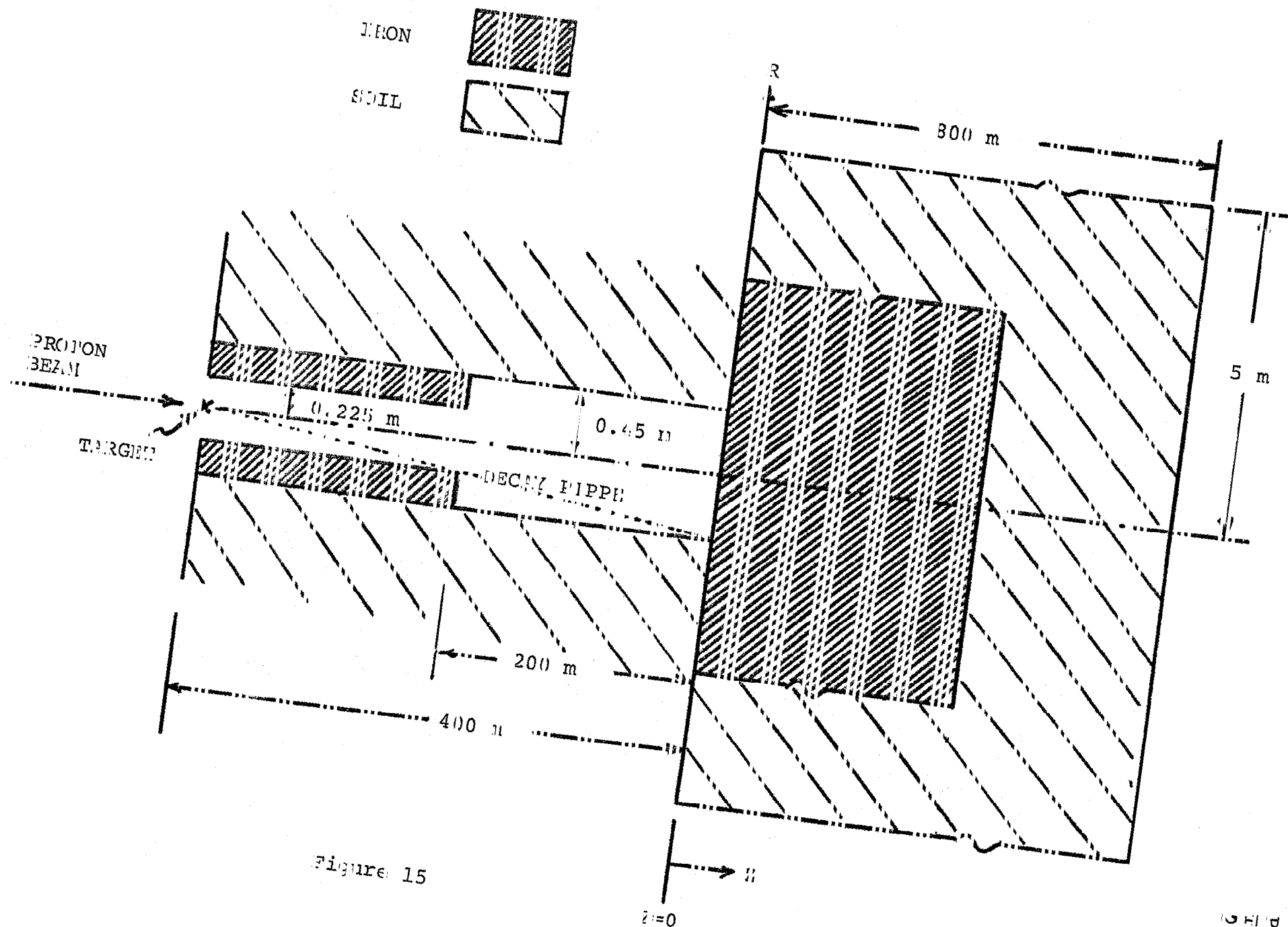


Figure 15

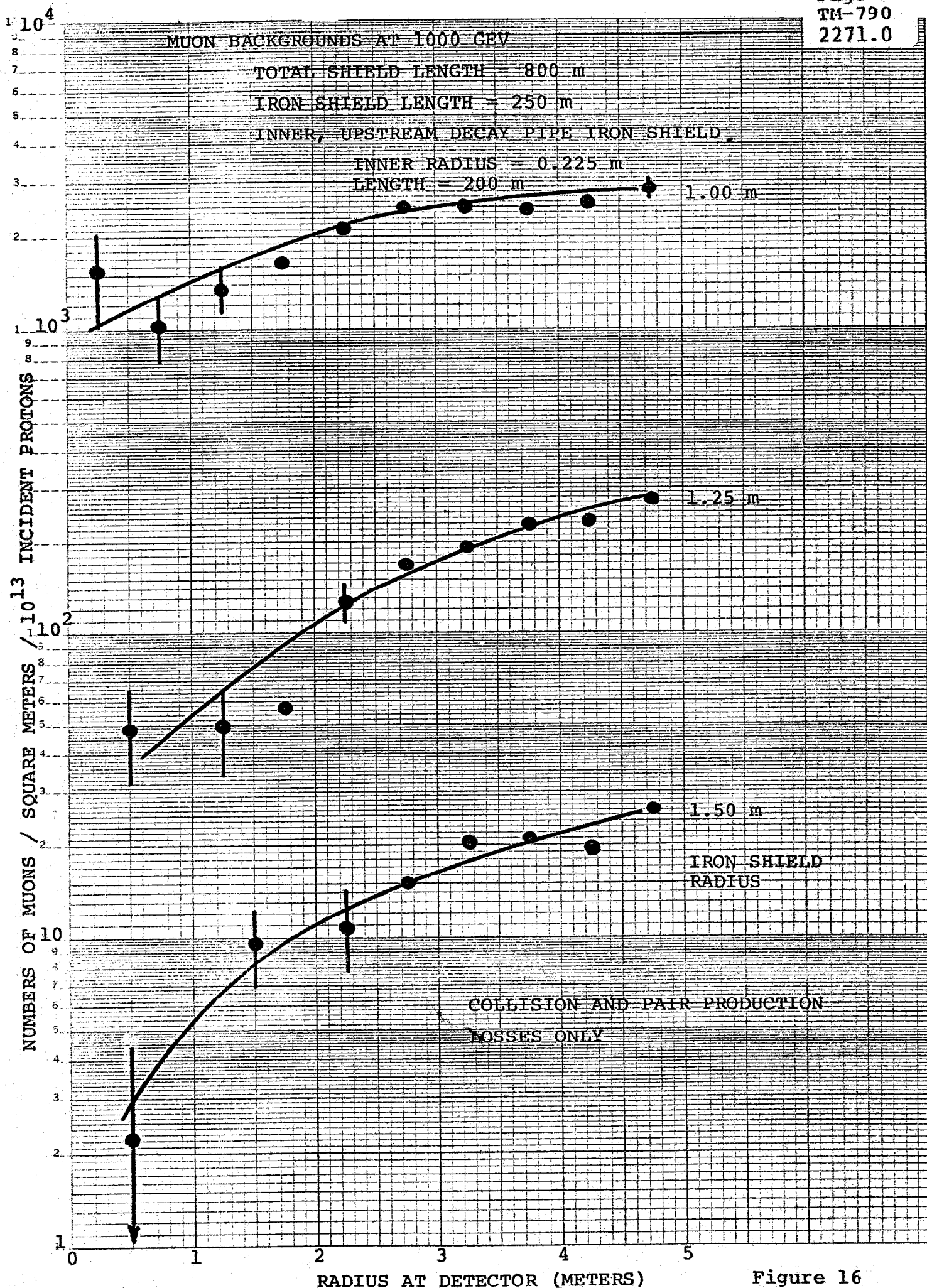


Figure 16

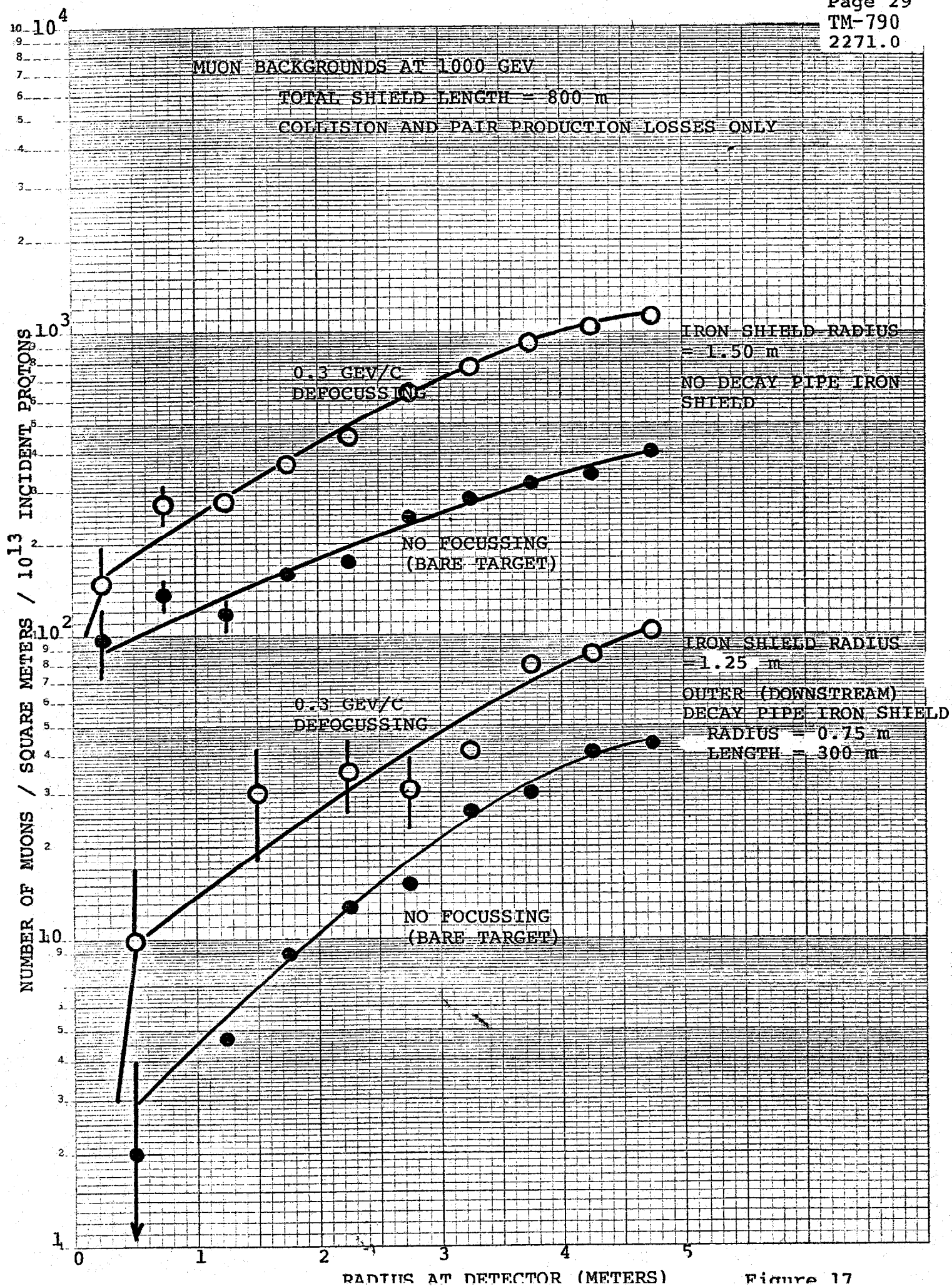


Figure 17